

# Multi-objective Optimization of Production Scheduling Using Particle Swarm Optimization Algorithm for Hybrid Renewable Power Plants with Battery Energy Storage System

Jon Martinez-Rico, Ekaitz Zulueta, Ismael Ruiz de Argandoña, Unai Fernandez-Gamiz, and Mikel Armendia

**Abstract**—Considering the increasing integration of renewable energies into the power grid, batteries are expected to play a key role in the challenge of compensating the stochastic and intermittent nature of these energy sources. Besides, the deployment of batteries can increase the benefits of a renewable power plant. One way to increase the profits with batteries studied in this paper is performing energy arbitrage. This strategy is based on storing energy at low electricity price moments and selling it when electricity price is high. In this paper, a hybrid renewable energy system consisting of wind and solar power with batteries is studied, and an optimization process is conducted in order to maximize the benefits regarding the day-ahead production scheduling of the plant. A multi-objective cost function is proposed, which, on the one hand, maximizes the obtained profit, and, on the other hand, reduces the loss of value of the battery. A particle swarm optimization algorithm is developed and fitted in order to solve this non-linear multi-objective function. With the aim of analyzing the importance of considering both the energy efficiency of the battery and its loss of value, two more simplified cost functions are proposed. Results show the importance of including the energy efficiency in the cost function to optimize. Besides, it is proven that the battery lifetime increases substantially by using the multi-objective cost function, whereas the profitability is similar to the one obtained in case the loss of value is not considered. Finally, due to the small difference in price among hours in the analyzed Iberian electricity market, it is observed that low profits can be provided to the plant by using batteries just for arbitrage purposes in the day-ahead market.

Manuscript received: September 12, 2019; accepted: July 23, 2020. Date of CrossCheck: July 23, 2020. Date of online publication: October 22, 2020.

The authors would like to thank the scientific illustrator and designer Patricia Nagashiro for the illustration of Fig. 2.

This article is distributed under the terms of the Creative Commons Attribution 4.0 International License (<http://creativecommons.org/licenses/by/4.0/>).

J. Martinez-Rico (corresponding author), I. R. de Argandoña, and M. Armendia are with the Automation and Control Unit, Fundación Tekniker, Basque Research and Technology Alliance (BRTA), Iñaki Goenaga, 5, 20600 Eibar, Spain, and J. Martinez-Rico is also with the University of the Basque Country, Ing. Torres Quevedo, 1, 48013 Bilbao, Spain (e-mail: [jon.martinez@tekniker.es](mailto:jon.martinez@tekniker.es); [ismael.ruiz@tekniker.es](mailto:ismael.ruiz@tekniker.es); [mikel.armendia@tekniker.es](mailto:mikel.armendia@tekniker.es)).

E. Zulueta is with the Department of Systems Engineering and Control, College of Engineering at Vitoria-Gasteiz, University of the Basque Country, Nieves Cano, 12, 01006 Vitoria-Gasteiz, Spain (e-mail: [ekaitz.zulueta@ehu.eus](mailto:ekaitz.zulueta@ehu.eus)).

U. Fernandez-Gamiz is with the Department of Nuclear and Fluid Mechanics, College of Engineering at Vitoria-Gasteiz, University of the Basque Country, Nieves Cano, 12, 01006 Vitoria-Gasteiz, Spain (e-mail: [unai.fernandez@ehu.eus](mailto:unai.fernandez@ehu.eus)).

DOI: 10.35833/MPCE.2019.000021

**Index Terms**—Battery energy storage system, energy arbitrage, hybrid renewable energy system, particle swarm optimization.

## I. INTRODUCTION

RENEWABLE energy sources (RESs) have become key solutions to reduce greenhouse gas emissions and fossil fuel dependency on energy production [1], [2]. However, the increasing integration of these power sources implies some challenges, due to their stochastic and intermittent nature, and the increasing production uncertainty. This uncertainty in turn leads to greater energy reserve volumes in order to maintain a balance between the production and consumption.

Considering the production variability, hybrid combinations of these alternative sources can become complementary, and therefore improve the performance of the generation plant. As an example, a combination between wind and solar energy appears to be interesting for a hybrid renewable energy system (HRES) due to their greater development compared with less mature RESs [3]-[5].

Besides, in order to introduce a larger number of RESs into the power grid, the deployment of energy storage systems (ESSs) becomes a key point for the purpose of compensating the production intermittency, as well as for enhancing the profitability of renewable power plants [6]-[9]. There exist a wide range of storage technologies, which could be divided into capacity-oriented storage technologies (such as pumped hydroelectric or hydrogen storage systems) and access-oriented technologies (such as batteries, flywheels, and supercapacitors). The selection of them depends mostly on the desired capacity, power density, and response time. Considering these parameters, Li-ion technology appears as a great solution due to its suitable properties, namely fast response, high cycle life, high energy density, and high efficiency [10], [11].

Another fact that makes this technology attractive for its use is that the price of Li-ion batteries has dropped drastically in the last decade. This price drop is mainly attached to the development and rise in sales of electric cars, for which this technology is commonly applied. According to the last



survey published by Bloomberg New Energy Finance (BNEF) [12], the fall in price of battery packs is 85% between 2010 and 2018, from 1160 \$/kWh to 176 \$/kWh, and by 2024 the price could fall below 100 \$/kWh. This forecast is based on the relationship between the price and volume of batteries worldwide. From this analysis, BNEF has observed that every time the volume doubles, the price falls 18%, which implies that the battery price could be around 94 \$/kWh by 2024, and 62 \$/kWh by 2030.

The use of batteries brings multiple benefits to renewable plants, both in economic and technical aspects. A renewable plant can reduce deviations between firmed capacity and real production by using batteries, since batteries can provide the missing part when the HRES plant gives less power than expected. Likewise, when the plant produces more power than forecasted, the battery energy storage system (BESS) can store the energy surpluses. This fact, apart from being beneficial for the grid power management, also becomes economically beneficial for the plant, as penalties related to those differences are minimized. Moreover, an HRES is able to perform energy arbitrage by using an ESS, which consists in shifting energy from a certain moment to another. The aim of this strategy is to bid more energy when the price is higher, and to store energy in batteries when the price is lower, so that the benefits can be maximized [13], [14].

Furthermore, the use of batteries gives the HRES the opportunity to provide ancillary service such as frequency control and secondary reserve. Therefore, HRES can participate not only in energy markets, but also in the ancillary service markets [15]. This option has recently become a reality, as some countries such as Spain have accepted HRES in their legislation as ancillary service provider [16]. Therefore, many researches have been conducted in order to improve the participation of RES plants in both day-ahead and ancillary service electricity markets [17]-[19].

Several studies have previously optimized the production schedule of a power plant using an ESS for the day-ahead market. Nevertheless, most of them propose a single-objective optimization problem, which is usually linearized so that it can be solved with classical optimization methods [20]-[24].

In [20], a photovoltaic (PV) + battery system is optimized in order to determine the production schedule using a linear programming (LP) routine with an idealized system. Therefore, it does not consider neither the energy efficiency of the batteries, nor the degradation of them.

Similarly, in [21], an LP optimization is conducted with model predictive control (MPC) method in order to determine the optimal bidding of the plant. In the optimization process, ESS costs are considered, but the cost function does not take into account the energy losses that vary with the given power.

In [22], a stochastic/robust optimization model for optimizing the bidding strategy in both day-ahead and real-time markets is developed, but the model is proposed for a mixed-integer linear programming (MILP) optimization problem, and it does not take into account the nonlinear terms of the ESS.

Similarly, in [23], an MILP optimization is proposed for participating in arbitrage markets with batteries. Battery degradation is considered in the study, but in order to solve the optimization, the cost function has to be linearized.

Finally, in [24], a mixed-integer quadratic programming (MIQP) optimization is proposed for managing the operation of islanded microgrids and a battery degradation model is also considered. Nevertheless, as with MILP optimization, the objective function also has to be linearized in order to solve the problem.

In this paper, to improve the profits of an HRES, a day-ahead market participation optimization is developed for a plant consisting of wind turbines, PV modules, and a Li-ion ESS. The main contribution of this paper is to propose a production scheduling optimization methodology, which maximizes the profits obtained from performing the energy arbitrage, and minimizes the loss of value of the BESS at the same time. The loss of value is calculated considering both the loss of life with the change of its state of health (SOH), and the effect of the price drop with time. Furthermore, in contrast to other similar studies, energy efficiency of the battery is included into the cost function, which has a significant effect on the result.

## II. PRODUCTION AND PRICE ESTIMATION

The aim of this study is to optimize the participation of a hybrid renewable power plant into an electricity market in order to maximize its profits by applying energy arbitrage with the use of a BESS. For the present work, the Iberian electricity market has been selected, and therefore, some insights about the procedure carried out in this market should be remarked.

The Iberian electricity market is a liberalized market, in which different traders offer and buy energies in different sequential markets, and their offers are cleared depending on the price they bid. The first of these sequential markets, and the one to be optimized in this paper is the day-ahead market [25].

The day-ahead market is the core market among all the existing markets, as it is the main mechanism to conduct the electricity transactions. The majority of the electricity to be produced in the following day is sold and purchased in this market. It is composed of a single session, in which traders make their offers for each of the 24-hour periods of the following day (day  $D+1$ ). Traders send their offers to the Spanish Market Operator (MO), called OMIE, until 12 a.m. of day  $D$ , and after that, a complex algorithm clears the offers to decide which of them are accepted or refused.

An important point to consider is that, regardless of the price of each offer, there is going to be a common and unique price for each hourly period once the auction is finished. Therefore, renewable plants usually make their offers with a near-zero price in order to always be accepted. That is why all the energy offered by the plant is going to be considered as accepted in this study.

As for the price and production estimations used for this study, the following models are used.

### A. Price Estimation of Day-ahead Electricity Market

In order to conduct the optimization, the developed algorithm needs to consider certain prices for each hourly period of the day. As the main aim of the study is to present the benefits of conducting a multi-objective optimization, the price estimations used are going to be taken from real data published by the Spanish System Operator for year 2018 [26].

### B. Production Estimation

In real-time operation, wind power plants need to use weather forecasts to calculate the energy expected to be produced in the following hours, since the production offers are made a few hours before the real production time [25]. These forecasts usually have a certain degree of uncertainty, which leads to possible deviations between the expected production and real production. Nevertheless, in order to focus on the effects of conducting a multi-objective optimization for performing energy arbitrage, the forecasts are considered ideal in this study. As for the values considered, the ideal forecasts are made based on the real weather data. This simplification implies that there is going to be no penalties for failing to produce the expected energy.

Regarding the wind power estimation, the electricity produced by wind turbines is going to be calculated based on the  $P$ - $V$  curves of the wind turbines. As for the calculation, the wind speed values taken from the nearest weather station to the considered HRES are extrapolated to the hub height with the following equation [27]:

$$\frac{U(z)}{U(z_r)} = \left( \frac{z}{z_r} \right)^\alpha \quad (1)$$

where  $U(z)$  and  $U(z_r)$  are the wind speeds at the heights  $z$  and  $z_r$ , respectively; and  $\alpha$  is the power law exponent. To calculate  $\alpha$ , the equation proposed by Counihan [27] is used, which defines  $\alpha$  in terms of the surface roughness:

$$\alpha = 0.096 \lg z_0 + 0.016 (\lg z_0)^2 + 0.24 \quad (2)$$

For the studied case,  $z_0$  is taken as 0.1 m corresponding to a surface with few trees.

As for the solar power estimation, the energy produced with solar modules is calculated with (3):

$$P_{MPP} = P_{MPP,STC} [1 + \gamma (T_{cell} - 25)] \frac{G}{1000} \quad (3)$$

where  $P_{MPP}$  is the maximum power at a certain cell temperature  $T_{cell}$  and irradiance  $G$ ;  $P_{MPP,STC}$  is the maximum power at standard test conditions (STCs); and  $\gamma$  is the maximum power point (MPP) power coefficient of the module.

As for the cell temperature, its relationship with the ambient temperature  $T_{amb}$  can be expressed as:

$$T_{cell} = T_{amb} + (NOCT - 20) \frac{G}{800} \quad (4)$$

where  $NOCT$  is the temperature of the cell under nominal operating conditions ( $G=800$  W/m $^2$ ,  $T_{amb}=20$  °C,  $v_{wind}=1$  m/s), and  $v_{wind}$  is the wind velocity. The value of  $NOCT$  is usually given by the manufacturer in the datasheet of the solar module.

It should be noted that, to estimate the power, some as-

sumptions are made as follows.

- 1) All wind turbines are receiving the same wind speed, uniformly distributed along each wind turbine.
- 2) All solar modules are receiving the same irradiance, uniformly distributed along each solar module.
- 3) In both cases, generators are always working at their MPPs under the given conditions.
- 4) No losses are considered regarding the connections and transmission lines of the system.

### III. BATTERY MODEL

Regarding the BESS, a simple equivalent circuit model (ECM) consisting of an ideal voltage source and a series resistance has been used to model the static response of the batteries. This simplified model is used to obtain the energetic efficiency curves.

The energetic efficiency can be defined as the relationship between voltage source power (internal power of the battery  $P_{int}$ ) and the power in the terminals (external power  $P_{ext}$ ). Nevertheless, depending on the battery charging/discharging state, the equation changes as follows.

In charging case, the energetic efficiency  $\eta_{chg}(P_{int})$  is calculated as:

$$\eta_{chg}(P_{int}) = \frac{P_{int}}{P_{ext}} = \frac{OCV^2}{OCV^2 + R_s P_{int}} \quad (5)$$

In discharging case, the energetic efficiency  $\eta_{dis}(P_{int})$  is calculated as:

$$\eta_{dis}(P_{int}) = \frac{P_{ext}}{P_{int}} = \frac{OCV^2 - R_s P_{int}}{OCV^2} \quad (6)$$

where  $OCV$  is the open circuit voltage; and  $R_s$  is the series resistance.

In addition to modelling the energy efficiency, the SOH of the battery is also considered in this study. In many optimization studies, this parameter is not taken into account, but as it is going to be proved, it has an important effect on the final optimization result. The SOH refers to the current maximum capacity of the battery compared with its nominal capacity. The two main factors that affect the SOH are cycling (charging and discharging) and calendar aging. In this study, the SOH is calculated focusing on the cycling. The Wöhler method is selected to estimate SOH [28]. For applying this method, it is necessary to know the number of cycles that can be given in the battery for each depth of discharge (DOD) range. This information is usually given in the datasheets of the battery.

### IV. OPTIMIZATION OF PRODUCTION SCHEDULE

As explained before, the HRES plant is capable of performing energy arbitrage by using a storage system. Therefore, the optimization includes offering a certain quantity of energy each hour in order to make as many profits as possible based on generation forecasts and price estimations for day  $D+1$ .

#### A. Cost Function

One of the benefits of the battery system incorporated to

the hybrid plant is that wind turbines and solar panels can be expected to work at their MPPs regardless of the power schedule of the plant, as the batteries should be able to damp those differences.

Therefore, considering the forecasting production as the real production, wind and solar productions are constant values for the cost function, and the target is to optimize the battery deployment.

The proposed objective function is defined for a multi-objective optimization problem, as it covers two main aims. The first aim is to optimize the battery use in order to maximize the profit of the plant, and the second aim is to minimize the loss of value of the battery due to using it.

As for the second aim, two factors are taken into account to calculate the loss of value of the battery.

On one hand, the SOH of the battery is considered in terms of the loss of life each day. In order to calculate the loss of life of the battery, a fatigue model known as Wöhler method is selected [28]. Fatigue models are commonly used for forecasting the aging of mechanical elements. These models consider that the analyzed element degrades step by step according to its use. Therefore, for the case of the BESS, the model does not consider the physico-chemical reactions given inside the battery, and treats the battery as a mechanical element instead. The Wöhler method has been selected due to its simplicity to be implemented and its sufficient accuracy in order to estimate the real SOH of the battery [21], [29], [30]. This method calculates the loss of life given in the battery ( $LL$ ) by (7) and (8):

$$LL = \sum_{i=1}^{n_{ranges}} LL_i \quad (7)$$

$$LL_i = \frac{n_{cycles}^i}{N_{cycles}^i} \quad (8)$$

where  $LL_i$  is the loss of life at a certain DOD range;  $n_{ranges}$  is the number of ranges into which the depth of discharge is divided;  $n_{cycles}^i$  is the number of cycles given at the  $i^{\text{th}}$  DOD range; and  $N_{cycles}^i$  is the maximum number of cycles at the  $i^{\text{th}}$  DOD range.

When  $LL$  reaches a value of 1, it means the battery has reached its end of life. Therefore, it is also possible to calculate the battery lifetime left by the following equation:

$$LT = \frac{1}{LL_{year}} \quad (9)$$

where  $LT$  is the lifetime years; and  $LL_{year}$  is the loss of life given in a complete year.

As for the number of fatigue cycles in a certain period, since the cycles are not cyclical and do not have constant amplitudes, determining the number of them requires a specific method. The method widely used for this purpose is known as the Rainflow cycle counting algorithm, which is used for extracting cycles from a complex load history, and organizing them depending on their mean values and amplitudes [31].

For the battery case, the parameter analyzed to determine the given number of cycles is the state of charge (SOC) of the battery during a certain period. A cycle describes the

charging and discharging of the battery, and the cycles are classified depending on their DODs.

There exist some different types of Rainflow cycle counting algorithms, and the one chosen for this study is the three-point method for a nonperiodic load time history. This method is more efficient computationally than other methods, and it can be used in applications of real-time cycle counting [31].

On the other hand, apart from the SOH, the other parameters considered in this study for calculating the loss of value in the battery is the change of market price. As previously explained, the battery price has fallen drastically in the last decade, and the trends indicate that the price is going to keep decreasing.

As shown in Fig. 1, an exponential curve is obtained for estimating the Li-ion battery pack price based on the data published in the latest new energy outlook [12].

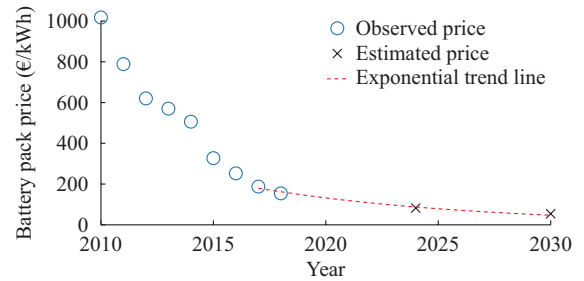


Fig. 1. Exponential trend of battery pack price.

The exponential curve estimates the unit price ( $UP$ ) for the battery in energy terms can be calculated as:

$$UP_{day} = 162.3e^{-0.1029d/365} \quad (10)$$

where  $UP_{day}$  is the unit price of a certain day; and  $d$  is the number of the days analyzed starting from January 1, 2018.

The curve has been obtained by fitting the data from 2017 until 2030, using the estimations of the latest New Energy Outlook [12]. It should also be remarked that, in order to convert the units from dollars to euros, a rate of 1.14 \$/€ is used.

Considering the SOH of the battery in terms of the  $LL$  and the  $UP$ , the loss of value of the battery from one day to another is defined as:

$$LV_{bat} = E_{nom} (1 - LL_{tot,day}) \cdot UP_{day} - E_{nom} (1 - LL_{tot,day-1}) \cdot UP_{day-1} \quad (11)$$

where  $E_{nom}$  is the rated energy of the battery at the beginning of its life;  $LL_{tot,day}$  is the total cumulative loss of life after day  $D$ ; and  $LL_{tot,day-1}$  is the total cumulative loss of life at the end of day  $D-1$ .

Finally, the global multi-objective cost function to maximize at day  $D$  is ( $LV_{bat}$  is always zero or negative):

$$\max \left( \sum_{h=1}^{24} E_{give,h} \cdot FP_h + LV_{bat} \right) \quad (12)$$

where  $E_{give,h}$  is the total energy given at each hour; and  $FP_h$  is the forecasting price for each hour.

As explained before, the energy given by the battery is affected by its energy efficiency, and the efficiency curves are

different in charging and discharging cases. Therefore,  $E_{give,h}$  is going to have one of the following expressions for each of the hours.

In charging and discharging cases,  $E_{give,h}$  is given in (13) and (14), respectively.

$$E_{give,h} = E_{gen,h} + \frac{1}{\eta_{chg,h}} (E_{bat,h-1} - E_{bat,h}) \quad (13)$$

$$E_{give,h} = E_{gen,h} + \eta_{dis,h} (E_{bat,h-1} - E_{bat,h}) \quad (14)$$

where  $E_{gen,h}$  is the forecasting energy generation at each hour; and  $E_{bat,h}$  is energy at the battery at each hour. Energy efficiencies  $\eta_{chg,h}$  and  $\eta_{dis,h}$  are the ones defined in (5) and (6).

An important point to take into account is that, in order to extend the battery life, charging and discharging cycles should not overpass certain SOC limits. These limits correspond to the bounds of optimization variables, and they are expressed as:

$$E_{bat,min} \geq E_{nom} \frac{SOC_{min}}{100} \quad (15)$$

$$E_{bat,max} \leq E_{nom} \frac{SOC_{max}}{100} \quad (16)$$

where  $E_{bat,min}$  and  $E_{bat,max}$  are the minimum and maximum energies of the battery, respectively; and  $SOC_{min}$  and  $SOC_{max}$  are expressed in percentage, and for the studied case, the SOC range is taken between 20% and 80% [32] in a Li-ion battery system.

### B. Constraints

The first constraints to be considered in the storage system are the ones related to the maximum charging and discharging power of the battery, namely  $P_{bat,chg,max}$  and  $P_{bat,dis,max}$ . Considering an hour as a time step, power constraints can be expressed as energy constraints with the following inequalities:

$$E_{bat,h} - E_{bat,h-1} \leq P_{bat,chg,max} h \quad (17)$$

$$E_{bat,h-1} - E_{bat,h} \leq P_{bat,dis,max} h \quad (18)$$

It should be noted that these maximum charging and discharging power values refer to the internal power given by the battery  $P_{int}$ . Therefore, as energy efficiency drops with the higher power, the efficiencies of giving or receiving the maximum internal power are the minimum efficiency values.

Secondly, in order not to make the battery at its lowest level at the end of the day, a constraint linked to the SOC at the last hour ( $E_{bat,24}$ ) is established. The aim is to keep the SOC of the battery similar to the one at the beginning of the day, and in order not to create an equality constraint, two inequality constraints are modelled as:

$$E_{bat,24} \geq \frac{SOC_{24,min}}{100} E_{nom} \quad (19)$$

$$E_{bat,24} \leq \frac{SOC_{24,max}}{100} E_{nom} \quad (20)$$

where  $SOC_{24,min}$  and  $SOC_{24,max}$  are the minimum and maximum SOCs of the battery at the last hour, respectively. For the simulations, the values assigned are 55% and 65%, respectively.

Finally, in the studied case, it is considered that batteries can only be charged with the HRES plant and cannot get energy directly from the power grid. This implies that the maximum charging value of the battery in an hour is limited by the energy generated, which is expressed as:

$$E_{bat,h-1} - E_{bat,h} \leq E_{gen,h} \eta_{chg} (E_{gen,h}) \quad (21)$$

where  $\eta_{chg}(E_{gen,h})$  is the charging efficiency for each  $E_{gen,h}$ .

In order to obtain a solution which meets all the constraints, for each constraint that is not fulfilled, a penalty is applied to the cost function. In this way, the solutions without any constraint violation obtain a better fitness.

### C. Optimization Algorithm

In order to solve the optimization problem, a particle swarm optimization (PSO) algorithm has been developed. This algorithm comes from the family of heuristic algorithms, which are widely used to solve complex multi-objective and non-linear problems [33]-[35]. It is developed by Kennedy and Eberhart in 1995 [36] based on swarm behaviors such as fish and birds schooling in nature.

To solve the optimization problem, the algorithm uses a set of particles. These particles are different possible solutions for the problem, and for this case, each of them is a vector with 24 components (energy of the battery at the end of each hour of the day). After creating the initial population of particles, the fitness of each of them is calculated, and the best global and local solutions are stored for the following iterations.

Depending on the fitness of each of the particles, the values of its components change with a certain speed (they move their positions). The particles which are far from the best solution move faster, and the ones which have a better fitness move slower.

The speed  $v_i$  and position  $x_i$  of each particle  $i$  are defined as:

$$v_i(t+1) = w_i(t+1)v_i(t) + \varphi_1(x_{i,best}(t) - x_i(t)) + \varphi_2(x_{best}(t) - x_i(t)) \quad (22)$$

$$x_i(t+1) = x_i(t) + dt \cdot v_i(t) \quad (23)$$

where  $w_i(t)$  is the inertia of the  $i^{\text{th}}$  particle at iteration  $t$ ;  $x_i(t)$  is the  $i^{\text{th}}$  particle position at iteration  $t$ ;  $x_{i,best}(t)$  is the local best position of the  $i^{\text{th}}$  particle at iteration  $t$ ;  $x_{best}(t)$  is the global best position at iteration  $t$ ;  $\varphi_1$  and  $\varphi_2$  are the uniform random values for the exploration and exploitation, respectively; and  $dt$  is the position update term.

As for the initial population of particles, i.e., the initial possible solutions for the optimization problem, more than one initialization method is used in order to assure that a profitable solution is found.

Firstly, the PSO algorithm is run with a completely random initial population in order to cover the solution domain and find the best solution. Nevertheless, it could happen that the PSO algorithm does not find a solution which fulfills all the constraints, or that the solution found is not profitable.

To solve this issue, the PSO algorithm is run a second time with a new initialization method. Here, the initial population is composed of random particles as well, but one of

the particles corresponds to the solution obtained for a simplified cost function. This solution is calculated by an LP algorithm.

LP is a powerful optimization technique when the cost function and constraints of the problem are linear [18]. Therefore, in order to solve the problem with this technique, the simplified cost function does not consider neither the energy efficiencies, nor the loss of value of the battery, and it is expressed as:

$$\max \sum_{h=1}^{24} [E_{gen,h} + (E_{bat,h-1} - E_{bat,h})] \cdot FP_h \quad (24)$$

The solution obtained by both initialization methods is compared, and the solution with a better fitness is chosen as the result for the multi-objective optimization problem.

Nevertheless, as explained in the next section, applying energy efficiencies to the solution obtained with the simplified cost function, the profit could be less than those of others without the ESSs. Therefore, as a definitive way to assure that a profitable solution is always found, a third initialization method is used if needed. The third method is similar to the second one (LP particle + random particles), but a new particle is introduced into the initial population. This new particle keeps the battery SOC at its initial value during the complete day so that a non-negative profit is assured.

## V. CASE STUDY

As explained before, in the present study, a grid-connected HRES consisting of wind turbines, solar modules, and Li-ion batteries is considered.

A graphical representation of the plant is shown in Fig. 2.



Fig. 2. Graphical representation of hybrid renewable power plant.

The sizing of the power plant considered for the simulations is as follows: 50 MW of wind power, 30 MW of solar power, and 10 MW/50 MWh of battery. For conducting the simulations, WindPACT baseline 1.5 MW wind turbines [37], developed by the National Renewable Energies Laboratory (NREL), have been considered. As for PV modules, the datasheet of Atersa ULTRA A-255 solar modules has been used [38].

Regarding the BESS, the data for the LiFeBATT X-2E 15 Ah 40166 Cell are used in order to parametrize the model as shown in Table I, and the results are adjusted to the case power range.

The resulting curves for different power values (maximum external power value  $P_{ext,max}$  is 10 MW) are calculated based on (5) and (6), and the result is shown in Fig. 3.

In order to get the same  $P_{ext,max}$ , the maximum internal power  $P_{int,max}$  is different for charging and discharging cases.

Besides, it should be pointed that  $R_s$  is considered as constant during the simulation.

TABLE I  
DATA TAKEN FROM DATASHEET FOR LiFeBATT X-2E 15AH 40166 Li-ION CELL

| Parameter | Value |
|-----------|-------|
| $OCV$     | 3.3 V |
| $R_s$     | 3 mΩ  |
| $I_{max}$ | 45 A  |

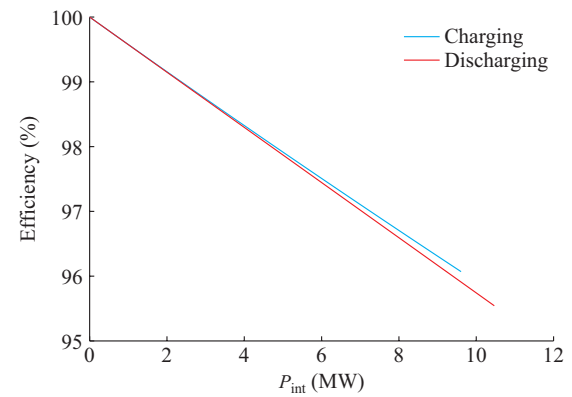


Fig. 3. Efficiency curves for the studied BESS.

As for the battery Wöhler curve, the values used are taken from [39], which are summarized in Table II.

TABLE II  
NUMBER OF CYCLES ADMITTED BY EACH DOD RANGE

| DOD range (%) | DOD interval (%) | Number of cycles |
|---------------|------------------|------------------|
| 10            | 5-15             | 70000            |
| 20            | 15-25            | 31000            |
| 30            | 25-35            | 18100            |
| 40            | 35-45            | 11800            |
| 50            | 45-55            | 8100             |
| 60            | 55-65            | 5800             |
| 70            | 65-75            | 4300             |
| 80            | 75-85            | 3300             |
| 90            | 85-100           | 2500             |

## VI. SIMULATION SETUP AND RESULT

In order to analyze the effects of performing energy arbitrage in a representative period, the data of a complete year have been simulated. The data in 2018 are taken from the data published by the Spanish System Operator for price values [26], and from the Basque Meteorological Agency Euskalmet [40] for forecasting calculation. In this case, the plant is supposed to be located in the Province of Álava, in the North of Spain.

Before analyzing the effects of the battery in the economic revenues, the parameters of the PSO have been fitted by an iterative method. In the case of the PSO, the inertia is considered as the main parameter affecting the final solution, so the rest of the parameters are fitted as constant, with the

values in Table III.

TABLE III  
FIXED PARAMETERS FOR PSO ALGORITHM

| Parameter            | Value or interval |
|----------------------|-------------------|
| $\varphi_1$          | 0.5-1             |
| $\varphi_2$          | 0.5-1             |
| $dt$                 | 1                 |
| Number of particles  | 200               |
| Number of iterations | 2000              |

As for the inertia, there exists a wide range of methods to calculate it [41]. Three methods, namely the random method, the linear time-varying method, and the adaptive method, have been tried and compared for recalculating the inertia during the optimization [41]. The results obtained for a particular day in 100 simulations with different seeds are shown in Fig. 4.

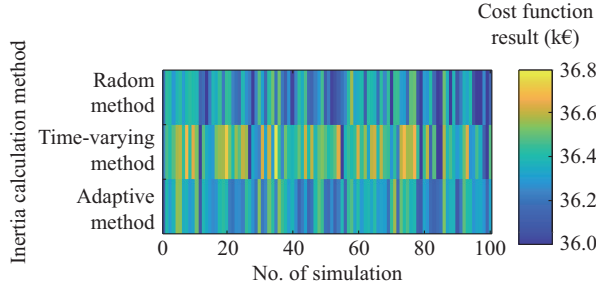


Fig. 4. Profit obtained by different inertia calculation methods.

As it can be seen in Fig. 4, time-varying method has better results in most cases. On average, the cost function results of time-varying method are 0.3% and 0.4% higher than adaptive and random methods, respectively. Therefore, it is going to be the method selected for the algorithm.

After fitting the parameters, simulations are conducted for the complete year. Each day is optimized and simulated consecutively, following the real-time schedules of the Iberian Electricity Market.

In order to analyze the effects of performing a multi-objective optimization, three different cost functions have been tested.

1) Multi-objective cost function is solved with PSO, namely PSOMO, as defined in (12).

2) Single-objective cost function is solved with PSO, not considering the loss of value of the battery, namely PSOSO. The function is:

$$\max \sum_{h=1}^{24} E_{\text{give},h} \cdot FP_h \quad (25)$$

3) Simplified objective function is solved with LP, not considering neither the loss of value of the battery, nor the energy efficiencies, as defined in (24).

As for the mean computation time, based on the parameters from Table III, and an Intel Core i5 CPU with 8 GB of RAM, each LP optimization takes less than 1 s, and PSOSO and PSOMO optimization take about 30 s and 65 s, respec-

tively.

Figure 5 shows the net profitability considering energy efficiencies, which is obtained for each day with the proposed cost functions. As it can be observed, by using the simplified cost function, the net profitability obtained is negative in a considerable number of days. This is due to the fact that if the energy losses are neglected, the ESS tends to be used with more and deeper charging and discharging cycles, which considers real energy losses and implies a higher loss of energy. This effect can be observed in Fig. 6, where the total number of cycles during the year for each DOD range are shown.

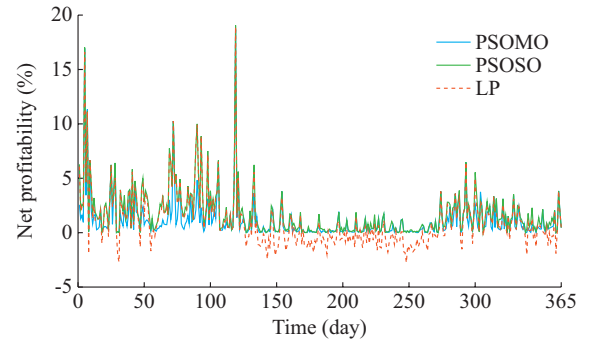


Fig. 5. Net profitability obtained for each day with different cost functions.

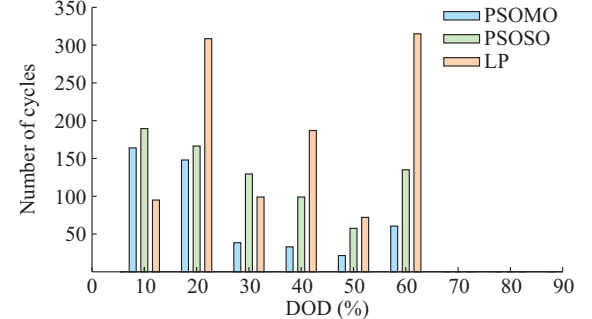


Fig. 6. Number of cycles for each DOD range with different cost functions.

It can be better understood that with neglecting energy efficiency, the profit obtained would be negative by analyzing a single day case.

Figures 7 and 8 show the solution obtained for Day 259 of the year (September 16, 2018), and Table IV shows the profitability results obtained with different cost functions. As it can be observed, LP solution creates more and deeper energy cycles, which would lead to a higher profit. Nevertheless, the results show that the net profitability obtained is negative by applying energy efficiencies, and recalculating the real net profits.

Another aspect shown in Fig. 8 is that in all cases, the stored energy in the battery  $E_{\text{sto,bat}}$  does not exceed the energy produced by the plant. Thus, constraint (21) is fulfilled.

Besides, it is also observed that the net profitability obtained with PSOSO is higher than with PSOMO in most cases as it can be shown in Fig. 9.

This result is consistent considering that the PSOMO also

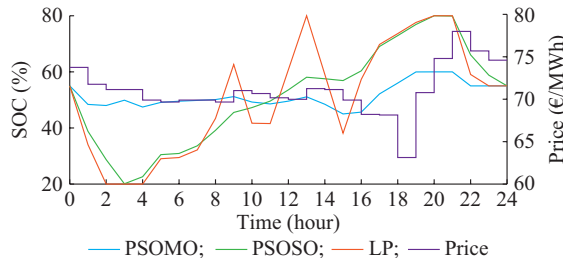


Fig. 7. Curves of SOC obtained on Day 259 with different cost functions and forecasting price of day-ahead electricity market.

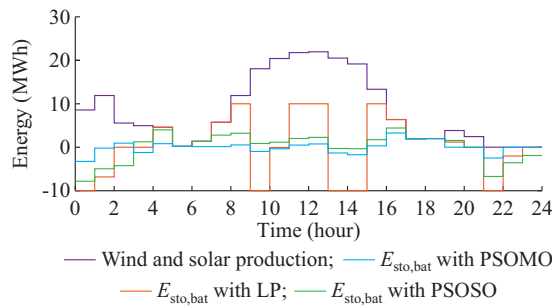


Fig. 8. Hourly wind and solar production and stored energy in the battery on Day 259 with different cost functions.

TABLE IV  
PROFITABILITY RESULTS OBTAINED WITH DIFFERENT COST FUNCTIONS ON  
DAY 259

| Cost function | Gross profitability (%) | Net profitability (%) |
|---------------|-------------------------|-----------------------|
| PSOMO         | 0.42                    | 0.32                  |
| PSOSO         | 1.03                    | 0.50                  |
| LP            | 1.44                    | -0.78                 |

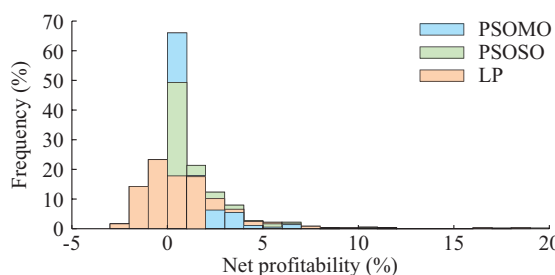


Fig. 9. Net profitability histograms with different cost functions.

tries to optimize the battery lifetime. Therefore, it is necessary to analyze both the net profitability and lifetime in a complete year to perform a complete comparison. The results are shown in Table V.

The results in a complete year show that performing the

TABLE V  
MEAN NET PROFITABILITY AND LIFETIME WITH DIFFERENT COST  
FUNCTIONS

| Cost function | Mean net profitability (%) | Lifetime (year) |
|---------------|----------------------------|-----------------|
| PSOMO         | 1.13                       | 39.80           |
| PSOSO         | 1.69                       | 18.52           |
| LP            | 1.05                       | 10.44           |

optimization with the multi-objective cost function, the battery lifetime is extended considerably, and in contrast, mean net profitability is similar to the one obtained with the single objective strategy. Besides, in both cases, the mean net profitability and lifetime are improved compared with the LP cost function result. Presumably, the real battery lifetime is less than the value obtained with these cost functions, since calendar aging is not included. Nevertheless, it is proven that the SOH associated to the cycling of the battery is significantly reduced with PSOMO method, while the mean net profitability is still better than in the LP case. Therefore, based on the multi-objective PSO strategy, global results are better than in the rest of the cases.

## VII. CONCLUSION

In this paper, a production scheduling optimization for the day-ahead market is conducted in an HRES plant with a BESS.

The main aim of this study is to analyze the importance of applying a multi-objective optimization to schedule the production. The multi-objective cost function optimizes both the net profitability of the plant and the loss of value of the battery, which are calculated with the number of cycles and the change of market price.

After simulating the data of a complete year, it can be seen that the global performance and profit of the plant are improved by implementing a PSO algorithm. In contrast, if the effects of the energy efficiency are neglected, the net profitability can be negative. Besides, it is proven that battery lifetime is substantially increased by using a multi-objective optimization, whereas the net profitability remains similar values.

Another conclusion is that the profitability is low by performing energy arbitrage uniquely in the day-ahead market. Benefits obtained from the arbitrage depend on price variation during the day, and in the Iberian Electricity Market, these differences are not substantial, nor are the benefits from it. Nevertheless, depending on price variations in each country, the profits could be significant.

Furthermore, it must be considered that production forecasts have been taken as ideal, and therefore there are no penalties for deviations in the production. Considering this aspect, the profits obtained with batteries could increase substantially, as batteries would be able to damp the differences between the forecasting and real production.

A last point to remark is that by participating in providing ancillary services with the ESS, the profits could increase considerably. This is a topic to be tackled in future works.

## REFERENCES

- [1] B. V. Mathiesen, H. Lund, and K. Karlsson, "100% renewable energy systems, climate mitigation and economic growth," *Applied Energy*, vol. 88, no. 2, pp. 488-501, Feb. 2011.
- [2] J. Pekez, L. Radovanovic, E. Desnica *et al.*, "The increase of exploitability of renewable energy sources," *Energy Sources, Part B: Economics, Planning, and Policy*, vol. 11, no. 1, pp. 51-57, Mar. 2016.
- [3] Q. H. Alsafafreh, "Performance and feasibility analysis of a grid interactive large scale wind/PV hybrid system based on smart grid methodology case study South Part - Jordan," *International Journal of Renewable Energy Development*, vol. 4, no. 1, pp. 39-47, Feb. 2015.

[4] H. Yang, L. Lu, and W. Zhou, "A novel optimization sizing model for hybrid solar-wind power generation system," *Solar Energy*, vol. 81, no. 1, pp. 76-84, Jan. 2007.

[5] A. Ugurlu and C. Gökçöl, "A case study of PV-wind-diesel-battery hybrid system," *Journal of Energy Systems*, vol. 1, no. 4, pp. 138-147, Oct. 2017.

[6] P. Denholm, E. Ela, B. Kirby *et al.* (2010, Jan.). The role of energy storage with renewable electricity generation. [Online]. Available: <https://www.osti.gov/biblio/972169-1QXROM/>

[7] N. Altin and S. E. Eyimaya, "A combined energy management algorithm for wind turbine/battery hybrid system," *Journal of Electronic Materials*, vol. 47, no. 8, pp. 4430-4436, Aug. 2018.

[8] K. Buss, P. Wrobel, and C. Doetsch, "Global distribution of grid connected electrical energy storage systems," *International Journal of Sustainable Energy Planning and Management*, vol. 9, pp. 31-56. Mar. 2016.

[9] B. Li, X. Li, X. Bai *et al.*, "Storage capacity allocation strategy for distribution network with distributed photovoltaic generators," *Journal of Modern Power Systems and Clean Energy*, vol. 6, no. 6, pp. 1234-1243, Nov. 2018.

[10] J. Leadbetter and L. G. Swan, "Selection of battery technology to support grid-integrated renewable electricity," *Journal of Power Sources*, vol. 216, pp. 376-386, Oct. 2012.

[11] T. Xu, W. Wang, M. L. Gordin *et al.*, "Lithium-ion batteries for stationary energy storage," *The Journal of the Minerals, Metals & Materials Society*, vol. 62, pp. 24-30, Sept. 2010.

[12] Bloomberg New Energy Finance. (2019, Jul.). New energy outlook 2019. [Online]. Available: <https://about.bnef.com/new-energy-outlook-2019/>

[13] K. Bradbury, L. Pratson, and D. Patiño-Echeverri, "Economic viability of energy storage systems based on price arbitrage potential in real-time U.S. electricity markets," *Applied Energy*, vol. 114, pp. 512-519, Feb. 2014.

[14] Y. Dvorkin, R. Fernandez-Blanco, D. S. Kirschen *et al.*, "Ensuring profitability of energy storage," *IEEE Transactions on Power Systems*, vol. 32, no. 1, pp. 611-623, Jan. 2017.

[15] J. Cho and A. N. Kleit, "Energy storage systems in energy and ancillary markets: a backwards induction approach," *Applied Energy*, vol. 147, pp. 176-183, Jun. 2015.

[16] Ministry of Industry, Energy and Tourism. (2015, Dec.). Criteria for participating in ancillary services. [Online]. Available:

[17] Y. Riffonneau, S. Bacha, F. Barruel *et al.*, "Optimal power flow management for grid connected PV systems with batteries," *IEEE Transactions on Sustainable Energy*, vol. 2, no. 3, pp. 309-320, Jul. 2011.

[18] M. Rahimiany and L. Baringo, "Strategic bidding for a virtual power plant in the day-ahead and real-time markets: a price-taker robust optimization approach," *IEEE Transactions on Power Systems*, vol. 31, no. 4, pp. 2676-2687, Jul. 2016.

[19] M. Chazarra, J. García-González, J. I. Pérez-Díaz *et al.*, "Stochastic optimization model for the weekly scheduling of a hydropower system in day-ahead and secondary regulation reserve markets," *Electric Power Systems Research*, vol. 130, pp. 67-77, Jan. 2016.

[20] A. Nottrott, J. Kleissl, and B. Washom, "Energy dispatch schedule optimization and cost benefit analysis for grid-connected, photovoltaic-battery storage systems," *Renewable Energy*, vol. 55, pp. 230-240, Jul. 2013.

[21] A. Gonzalez-Garrido, A. Saez-de-Ibarra, H. Gaztanaga *et al.*, "Annual optimized bidding and operation strategy in energy and secondary reserve markets for solar plants with storage systems," *IEEE Transactions on Power Systems*, vol. 34, no. 6, pp. 5115-5124, Nov. 2019.

[22] G. Liu, Y. Xu, and K. Tomsovic, "Bidding strategy for microgrid in day-ahead market based on hybrid stochastic/robust optimization," *IEEE Transactions on Smart Grid*, vol. 7, no. 1, pp. 227-237, Sept. 2016.

[23] H. C. Hesse, V. Kumtepeli, M. Schimpe *et al.*, "Ageing and efficiency aware battery dispatch for arbitrage markets using mixed integer linear programming," *Energies*, vol. 12, no. 6, p. 999, Mar. 2019.

[24] V. Kumtepeli, Y. Zhao, M. Naumann *et al.*, "Design and analysis of an aging-aware energy management system for islanded grids using mixed-integer quadratic programming," *International Journal of Energy Research*, vol. 43, no. 9, pp. 4127-4147, Jun. 2019.

[25] Ministry of Energy, Tourism and Digital Agenda. (2018, May). Day-ahead and intraday electricity market operating rules. [Online]. Available:

[26] Red Eléctrica de España. (2019, Aug.). System operator information system. [Online]. Available:

[27] J. F. Manwell, J. G. McGowan, and A. L. Rogers, *Wind Energy Explained: Theory, Design and Application*, 2nd ed. Chichester: John Wiley and Sons, 2010.

[28] D. U. Sauer and H. Wenzl, "Comparison of different approaches for lifetime prediction of electrochemical systems-using lead-acid batteries as example," *Journal of Power Sources*, vol. 176, no. 2, pp. 534-546, Feb. 2008.

[29] A. Saez-de-Ibarra, V. I. Herrera, A. Milo *et al.*, "Management strategy for market participation of photovoltaic power plants including storage systems," *IEEE Transactions on Industry Applications*, vol. 52, no. 5, pp. 4292-4303, Sept. 2016.

[30] R. Dufó-López, J. M. Lujano-Rojas, and J. L. Bernal-Agustín, "Comparison of different lead-acid battery lifetime prediction models for use in simulation of stand-alone photovoltaic systems," *Applied Energy*, vol. 115, pp. 242-253, Feb. 2014.

[31] Y. L. Lee and T. Tjhung, "Rainflow cycle counting techniques" in *Metal Fatigue Analysis Handbook*, Oxford, UK: Butterworth-Heinemann, 2012, pp. 89-114.

[32] L. Xu, F. Yang, M. Hu *et al.*, "Comparison of energy management strategies for a range extended electric city bus," in *Proceedings of the 31st Chinese Control Conference*, Nanchang, China, Jul. 2012, pp. 640-647.

[33] E. Zulueta, E. Kurt, Y. Uzun *et al.*, "Power control optimization of a new contactless piezoelectric harvester," *International Journal of Hydrogen Energy*, vol. 42, no. 28, pp. 18134-18144, Jul. 2017.

[34] F. Ekinci, T. Demirdelen, I. O. Aksu *et al.*, "A novel hybrid metaheuristic optimization method to estimate medium-term output power for horizontal axis wind turbine," *Proceedings of the Institution of Mechanical Engineers, Part A: Journal of Power and Energy*, vol. 233, no. 5, pp. 646-658, Aug. 2019.

[35] S. Shojaeian and E. S. Naeeni, "Probabilistic optimal sizing of PV units in a distribution network," *Applied Solar Energy*, vol. 50, no. 3, pp. 125-132, Jul. 2014.

[36] J. Kennedy and R. Eberhart, "Particle swarm optimization," in *Proceedings of ICNN'95 - International Conference on Neural Networks*, Perth, Australia, Nov. 1995, pp. 1942-1948.

[37] J. Rinker and K. Dykes (2018, Apr.). WindPACT reference wind turbines [Online]. Available:

[38] Atersa (2017, Apr.). Atersa photovoltaic module A-255M / A-260M / A-265M. [Online]. Available:

[39] V. I. Herrera, A. Saez-de-Ibarra, A. Milo *et al.*, "Optimal energy management of a hybrid electric bus with a battery-supercapacitor storage system using genetic algorithm," in *Proceedings of 2015 International Conference on Electrical Systems for Aircraft, Railway, Ship Propulsion and Road Vehicles (ESARS)*, Aachen, Germany, Mar. 2015, pp. 1-6.

[40] Eusko Jaurlaritza-Gobierno Vasco. (2020, Feb.). Open data euskadi - weather station measurements in 2019. [Online]. Available:

[41] A. Nickabadi, M. M. Ebadzadeh, and R. Safabakhsh, "A novel particle swarm optimization algorithm with adaptive inertia weight," *Applied Soft Computing Journal*, vol. 11, no. 4, pp. 3658-3670, Jun. 2011.

**Jon Martinez-Rico** received the B.Sc. degree in renewable energies engineering from the University of the Basque Country, Eibar, Spain, in 2017, and the M.Sc. degree in sustainable energy engineering from the University of the Basque Country, Bilbao, Spain, in 2018. He is currently working toward the Ph.D. degree at Tekniker, Eibar, Spain, and the University of the Basque Country, Bilbao, Spain. Since 2018, he has been employed as a Researcher at Tekniker in the Automation and Control Unit. His research interests include energy management of energy storage systems, integration of renewable energies into the electricity market, optimization algorithms, and control of renewable power plants.

**Ekaitz Zulueta** received the B.Sc. degree in electronic engineering from Mondragon University, Arrasate, Spain, in 1997, the M.Sc. degree in electrical engineering from Swiss Institute of Technology Lausanne, Lausanne, Switzerland, in 2000, and the Ph.D. degree in control engineering from the University of the Basque Country, Vizcaya, Spain, in 2005. From 2000 to 2002, he has been employed as a Research Engineer with Ideko, Elgoibar, Spain and Fagor Automation, Arrasate-Mondragon, Spain. Since 2002, he has been employed as a Lecturer with the University of the Basque Coun-

try, Vitoria-Gasteiz, Spain. His research interests cover a range of computational intelligence areas including image processing and wind turbines control.

**Ismael Ruiz de Argandoña** received the B.Sc. degree in electronic engineering from Mondragon University, Arrasate, Spain, in 1993, and the M.Sc. degree in electronic engineering from Staffordshire University, Staffordshire, UK, in 1995. He received the M.Sc. degree in automatic control and industrial electronics from Mondragon University, Mondragon, Spain, in 1999, and the Ph.D. degree in electric and electronic engineering from the same university, in 2017. He works in Tekniker since 1995 and leads the Automation and Control Unit since 2007. His research interests include on-shore and offshore wind turbines, machine tools, measuring machines, special machines, and scientific equipment with special emphasis in telescopes.

**Unai Fernandez-Gamiz** received the B.Sc. and M.Sc degrees in mechanical engineering from the University of the Basque Country, Vitoria-Gasteiz,

Spain, in 1999 and 2004, respectively, and the Ph.D. degree in the mechanics, fluids and aeronautics from the UPC-Barcelona, Barcelona, Spain, in 2013. Since 2008, he works as a Full Lecturer in the Department of Nuclear Engineering and Fluid Mechanics at the University of the Basque Country, Vitoria-Gasteiz, Spain. His research interests include renewable energy sources and applied computational fluids dynamics methods.

**Mikel Armendia** received the B.Sc., M.Sc., and Ph.D degrees in mechanical engineering from Mondragon University, Arrasate, Spain, in 2005, 2007, and 2011, respectively. He was a Visitor Researcher in reference institutions from the manufacturing research world like the Advanced Manufacturing Research Centre (AMRC) from Sheffield, UK, and the University of North Carolina, Charlotte, USA. Now, he works in the Automation and Control Unit of Tekniker, Eibar, Spain. He has experienced coordinating European Projects (Twin-Control). His research interests include mechanical system modelling and servo control adjustment.